Designing surface alloys with specific active sites

P.M. Holmblad [a], J. Hvolbæk Larsen [a], I. Chorkendorff [a], L. Pleth Nielsen [b], F. Besenbacher [b],
I. Stensgaard [b], E. Lægsgaard [b], P. Kratzer [a], B. Hammer [a,c] and J.K. Nørskov [a]

[a] *Center for Atomic-Scale Materials Physics, Department of Physics, Technical University of Denmark, DK-2800 Lyngby, Denmark*
[b] *Center for Atomic-Scale Materials Physics, Institute of Physics and Astronomy, University of Aarhus, DK-8000 Aarhus C, Denmark*
[c] *Joint Research Center for Atom Technology (JRCAT), 1-1-4 Higashi, Tsukuba, Ibaraki 305, Japan*

Received 30 April 1996; accepted 26 May 1996

This report describes a combined experimental and theoretical approach to the problem of designing surface alloys with specific chemical properties. Au–Ni(111) surface alloys were prepared and the distribution of active sites was determined by atomically resolved STM as a function of Au coverage. Using density functional theory the difference in activation energy for methane over the various sites was determined. The activity of the surface could be predicted directly by combining this information with the distribution of sites. Subsequent measurements of the activity proved this method to be quantitative and demonstrated that surface alloys with specific activity can be synthesized.

Keywords: active sites; surface alloys; STM; molecular beams; activation barriers

One of the ultimate goals of surface science is to be able to design – on the atomic scale – surfaces with particular catalytic properties. It has long been realized that alloying can modify the catalytic activity and selectivity of a metal significantly [1,2], and that alloy catalysts represent one of the most promising avenues towards new catalyst systems [3]. It is still an open question in alloy catalysis whether alloying just changes the distribution of islands of a given metal which otherwise retains its reactivity (the ensemble effect) [1,2,4], whether alloying changes the local bonding geometry (the structure effect) [5], or the alloying also modifies the reactivity of the metal atoms (the electronic or ligand effect) [6,7]. Another question in alloy catalysis is how to control the surface concentration of the metallic constituents. Segregation between the bulk and the surface will typically be strongly influenced by adsorption of the reactants and therefore depends on the reaction conditions. In the following we shall see how the chemical activity of the surface Ni atoms can be tuned almost continuously by alloying, and it will be demonstrated that a surface alloy with specific activity can be synthesized.

Recently, it has been shown that in some cases alloys form in the outermost surface layer from metals which are immiscible in the bulk [8]. The problem of transport between the bulk and the surface is thus much reduced compared to bulk alloys, and a fraction of a monolayer of one metal on another is enough to form a stable surface structure. Au deposited on Ni(111) constitutes such a system. Fig. 1 shows an STM topograph of a Ni(111) surface where ~10% of a monolayer (ML) of Au has been deposited by evaporation. Even though the heat of solution of Au in Ni is large and positive [9], the deposited Au does not form islands on the Ni(111) surface but alloys into the first Ni layer. This alloying takes place over the full range of Au coverages. For each coverage, the STM images can be used to get the distribution of Au and Ni atoms relative to each other. In the insert of fig. 1, we show the probabilities of finding Ni atoms with zero, $P_0(\theta_{Au})$, and one, $P_1(\theta_{Au})$, Au neighbors determined from different STM images at different Au coverages θ_{Au}. As discussed below, this information will form the basis for the modeling of the reactivity of the alloyed surface.

We will use methane dissociation as a test reaction to study the effect of surface alloying. Fig. 2 illustrates the calculated reaction path for a methane molecule dissociating over a clean Ni(111) surface. The lowest barrier is found for the molecule impinging right over one of the Ni atoms. After the dissociation both the adsorbed H atom and the methyl group are found in three-fold sites. The calculated energy along the path is shown in fig. 3. The process is highly activated, in agreement with experiments calculations study the effect of alloying on the dissociation process by exchanging one or two of the neighboring Ni atoms by Au atoms. We shall keep the reaction path fixed, which is a very good approximation when the influence of changing the environment is small. This is particularly true at the top of the barrier where the stationary property of the potential energy surface ensures that changes in the path only give rise to second-order changes in the minimum barrier. As the dissociation still proceeds over a Ni atom we effectively study only the *change* in Ni properties due to alloying. The results are also included in fig. 3. If one out of six Ni neighbors is substituted by an Au atom, the barrier for methane dissociation is calculated to have an increase of $\Delta E_1 = 16$ kJ/mol (0.17 eV). If the Ni atom has two Au

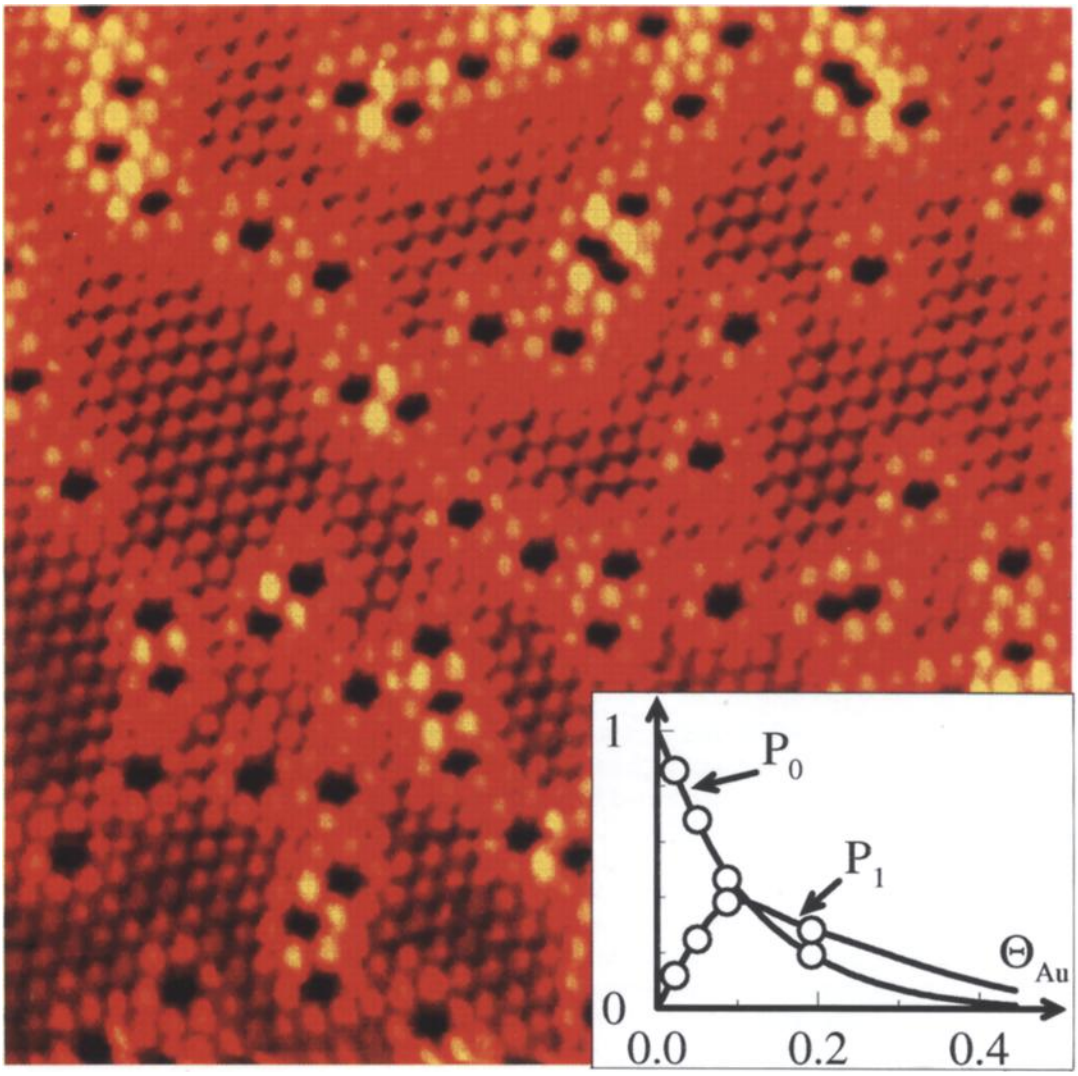

Fig. 1. Atom resolved STM topograph (75×75 Å^2) revealing the formation of an Au–Ni(111) surface alloy after deposition of 0.087 ML Au at 500 K. The substitutional Au atoms are seen as apparent holes (0.2 Å deep). Note how the six Ni atoms surrounding each substituted Au atom appear brighter. Our calculations show that the relaxations of the Ni atoms in the presence of Au neighbors are small. We therefore identify changes in the electronic structure of the Ni atoms next to Au atoms as the common reason for the brighter spots and the change in chemical reactivity of these atoms. The insert shows the probabilities $P_0(\theta_{\mathrm{Au}})$ and $P_1(\theta_{\mathrm{Au}})$ of finding a Ni atom with zero or one Au nearest neighbor as a function of the Au coverage in monolayers. The experimental points are fitted with smooth functions for the use in eq. (1). The probability distributions thus determined are very similar to those expected if the Au atoms were positioned at random.

neighbors, the barrier is increased by $\Delta E_2 = 38$ kJ/mol. More Au neighbors will increase the barrier even further. A full account of these calculations is given in ref. [17].

On the basis of these calculations it is reasonable to model the adsorption rate by assuming a sticking probability, s_N, per Ni site which only depends on the number, N, of Au nearest neighbors. A more sophisticated model would include more long range interactions, but these are expected to be considerably weaker. This is, for instance, illustrated by the STM image in fig. 1, where it is seen that the Ni atoms that are nearest neighbor to the Au atoms are affected much stronger than are Ni atoms further away from the Au. It is also seen that Ni atoms with two Au neighbors are more strongly affected than those with only one neighbor, providing further evidence that the number of Au nearest neighbors is the main factor determining the sticking probability. Given the probabilities, $P_N(\theta_{\mathrm{Au}})$, estimated from a series of STM measurements of finding a Ni atom with N Au neighbors at an Au coverage of θ_{Au} (see insert in fig. 1), we can get the sticking probability as

$$s(\theta_{\mathrm{Au}}) = s_0 \cdot P_0(\theta_{\mathrm{Au}}) + s_1 \cdot P_1(\theta_{\mathrm{Au}}) + s_2 \cdot P_2(\theta_{\mathrm{Au}}) + \dots \qquad (1)$$

We now want to test this model by comparing to experiment. In a thermal experiment we would approxi-

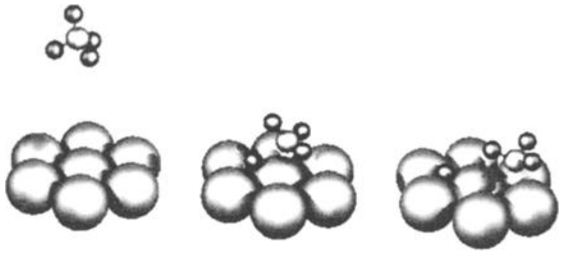

Fig. 2. An illustration of the dissociative adsorption of CH_4 on a Ni(111) surface. In the most favorable reaction path, the impact of the CH_4 on a Ni atom (large sphere) is close to the on-top position with the H (small dark sphere) and CH_3 group moving into opposite hollow sites. In the middle picture, the calculated transition state is shown. Here the C atom (medium sized, bright sphere) is located 2 Å above the surface and the active C–H bond is stretched to 1.6 Å, as compared to 1.08 Å in the CH_4 molecule.

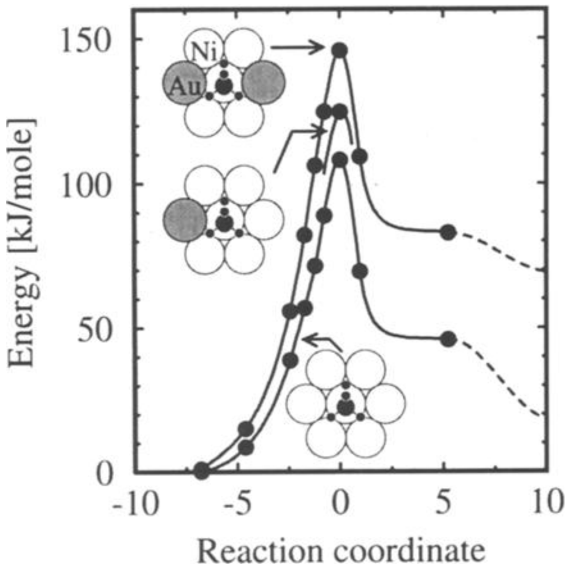

Fig. 3. The calculated energy along the reaction path for CH_4 dissociating over a Ni atom in the Ni(111) surface. Results from similar calculations for dissociation over a Ni atom with one or two Au nearest neighbors are also included. The Au atoms are gray-shaded in the plots indicating the dissociation geometry for the three cases. The geometries of the CH_4 along the reaction path include full structural relaxation of the CH_3 group in each step. The rightmost data points (dashed curves) refer to infinite separation of the dissociated H and CH_3 group on the surface. The calculations are done in a super cell geometry with CH_4 approaching one side of a Ni slab consisting of four atomic layers. The lateral periodicity is described by surface unit cells containing four Ni atoms, five Ni and one Au atom, or three Ni and one Au atom, for the three cases considered. For the Au–Ni system the Au and the surrounding Ni atoms have been allowed to relax, but the reaction path is kept the same as over clean Ni. The total energies are calculated within density functional theory [18] describing exchange and correlation effects in the local-density approximation augmented by non-local corrections in the so-called generalized gradient approximation (GGA) [19]. Corrections due to the zero-point energy of the transition complex, which are not included in the presented curves, will tend to lower the calculated barriers.

mately have that $s_N/s_0 = \exp(-\Delta E_N/kT)$ where ΔE_N is the difference in activation energy for a Ni site with N and one with no Au neighbors. We can, however, get a more detailed test by studying the methane dissociation rate using a beam of methane molecules specified by the translational energy E_T and the distribution of internal vibrational and rotational states (corresponding to the nozzle temperature T_{nozzle}). In fig. 4, we show the results from such a molecular beam experiment for methane dissociation over Ni(111) with varying amounts of Au on the surface. A full account of the molecular beam experiments is given in ref. [20]. Results are shown for two beams with approximately the same kinetic energy, but different nozzle temperatures. The uncertainties on the experimental data have been indicated with error bars. The high T_{nozzle} beam is more reactive due to a higher fraction of vibrationally excited molecules [12,13]. Since the calculation for the case of two Au neighbors shows a large increase in barrier, it is reasonable to neglect sticking on sites with more than one Au neighbor ($s_N = 0, N > 1$ in eq. (1)). We fit the expression for $s(\theta_{\mathrm{Au}})$ to the data in fig. 4, obtaining values for s_0 and s_1 for both the 1050 K beam ($s_0 = 1.2 \times 10^{-2}$, $s_1 = 3.1 \times 10^{-3}$ yielding $s_1/s_0 = 0.27$) and for the 550 K beam ($s_0 = 1.8 \times 10^{-3}$, $s_1 = 1.8 \times 10^{-12}$, yielding $s_1/s_0 = 10^{-9}$). In order to investigate the sticking on the Ni sites with one Au neighbor, we invest eq. (1) and plot in fig. 5 the experimental $(s(\theta_{\mathrm{Au}})/s_0) - P_0(\theta_{\mathrm{Au}})$ which, if the model is reasonable, is a measure for $s_1/s_0 \cdot P_1(\theta_{\mathrm{Au}})$. Uncertainties on these modified experimental data are shown for the 1050 K beam, while error bars in the same order of magnitude apply for the 550 K beam. Using the already obtained values for s_1 and s_0 and the expression for $P_1(\theta_{\mathrm{Au}})$, the solid lines are obtained. These are seen to describe the experimental data very well, clearly indicating that the assumptions and the model are reasonable.

For comparison of the theoretical calculation to the molecular beam experiments, we will as a first-order approximation assume that the effect on the sticking coefficient when increasing the barrier height, corresponds to decreasing the translational energy by an equivalent amount under otherwise similar conditions. Therefore, the reduced sticking probability, s_1/s_0, corresponding to dissociation over a site with one Au nearest neighbor having an increased barrier of 16 kJ/mol, can be found using the insert in fig. 4. Here, the initial sticking probability on Ni(111) has been shown for the two vibrational temperatures used in fig. 4 as a function of translational energy of the CH_4 molecule. For sites with a barrier ΔE_1 higher than for pure Ni(111), we therefore assume a reduced sticking of $s_1/s_0 = s_0(E_T - \Delta E_1)/s_0(E_T)$ at a given nozzle temperature T_{nozzle} and translational energy E_T. The increased barrier of $\Delta E_1 = 16$ kJ/mol corresponds to a reduced sticking probability of $s_1/s_0 = 0.23$ for the 1050 K beam and $s_1/s_0 = 0.07$ for the 550 K beam are obtained. Multiplying these numbers with $P_1(\theta_{\mathrm{Au}})$ the dashed lines in the insert in fig. 4 evolve. These are seen to describe the experimental data points

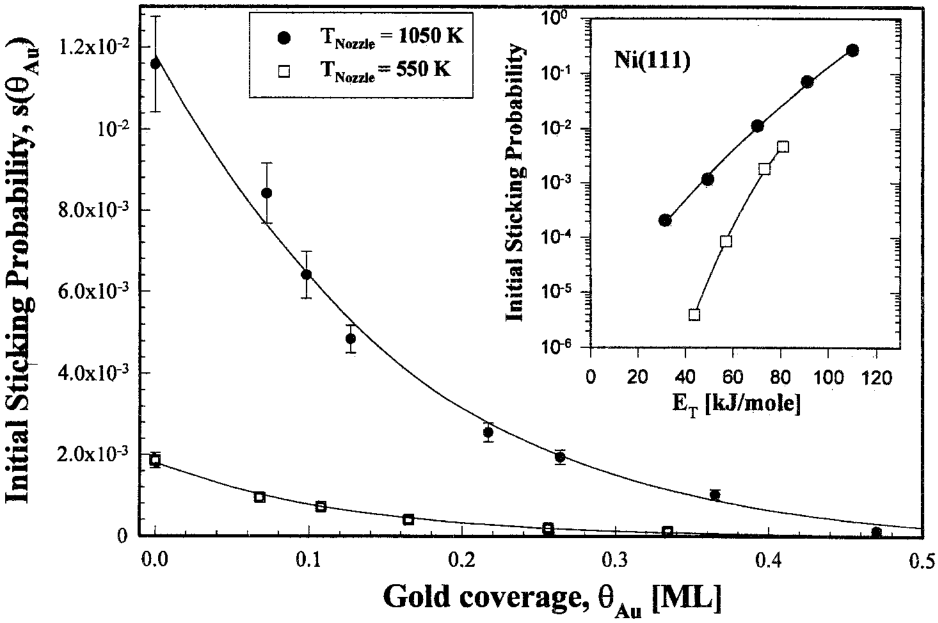

Fig. 4. The measured initial sticking coefficient of methane on the Au–Ni(111) surface is shown for two molecular beams with approximately the same translational energy (~75 kJ/mol), but with different nozzle temperatures (vibrational temperature). The absolute sticking probabilities are shown as a function of Au coverage. The values found are $s_1/s_0 = 0.27$ for the 1050 K beam and $s_1/s_0 = 0.00$ for the 550 K beam. The insert shows the measured sticking coefficients as a function of the beam energy over the pure Ni(111) surface for the two nozzle temperatures. This information is used to determine the dependence of the sticking probability on the barrier height. As a first-order approximation it is assumed that an increase in barrier height corresponds to a similar decrease in translational energy for the two beams. Hereby, the ratio of the sticking coefficients are expected by theory to be $s_1/s_0 = 0.23$ and $s_1/s_0 = 0.07$ for $T_{\text{nozzle}} = 1050$ and 550 K, respectively. The solid lines show the theoretical dependence given by eq. (1), where the sticking coefficients have been weighted by their appropriate probabilities $P_0(\theta_{\text{Au}})$ and $P_1(\theta_{\text{Au}})$.

well, clearly indicating that sites with one nearest neighbor Au atom do indeed have a reactivity, however reduced. Only the vibrationally excited methane molecules are able to surmount this barrier in measurable numbers. The good agreement with the theoretical predictions of the increased barrier should also be emphasized.

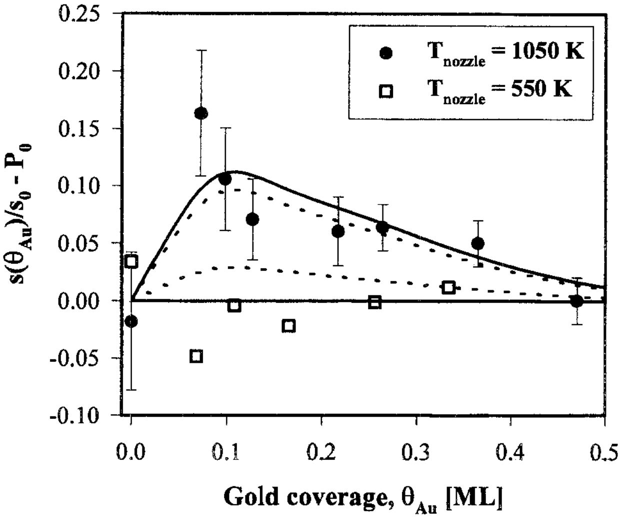

Fig. 5. The experimentally determined sticking probabilities shown in fig. 4 have been divided by s_0 and the function describing the number of sites with only Ni atoms as nearest neighbors, $P_0(\theta_{\text{Au}})$ has been subtracted. $P_0(\theta_{\text{Au}})$ has been determined from statistical work on STM pictures of the Au–Ni(111) surface. The solid lines are $s_1/s_0 \cdot P_1(\theta_{\text{Au}})$ using the parameters determined in fig. 4. The dashed lines describe the dependence expected from the theoretically calculated increase in barrier.

The implications of this work are threefold. First, it illustrates that the theoretical methods from density functional theory have reached a point where they can be used to predict trends in the chemical activity when a surface is modified by alloying. This opens up new prospects in computer aided design of catalysts. Second, it is clear that ensemble control is an important aspect of alloy catalysis, but the surface atoms of the alloy do not retain their clean metal properties even for a reaction which takes place over a single atom. This allows for a much more fine tuning of metal surface reactivity than the differences between the elemental metals offer. Finally, it shows that it is possible to synthesize and characterize new surface structures at the atomic level. These structures have no bulk counterpart and constitute a new set of possibilities in catalysis research.

In this work we have shown that it is possible to go all the way from synthesis of a surface alloy and subsequent measurement of the distribution of different sites to a prediction of its reactivity. The predictions have been tested by direct measurement. The success of this approach opens new possibilities in the "design" of surfaces with a specified reactivity. The results presented so far have dealt with surface alloys with a lower methane dissociation rate than for clean Ni(111). This is still of potential technological interest since selectivity is often more important than activity. Nickel catalysts used in the steam reforming process are for instance selectively poisoned by sulfur to prevent carbon formation [21]. The gold alloy could have the same effect of providing Ni ensembles that are not large enough for the incorporation of carbon into the catalyst. The activity of the Ni surface can, however, also be increased by alloying. Our calculations predict that Ni atoms surrounded by Cu atoms in the surface have a barrier for methane dissociation which is 0.05 eV lower than the clean Ni surface in accordance with experience from experiments on alloy catalysts [22].

Acknowledgement

The calculations have only been possible due to the computational resources of the JRCAT supercomputing system, which is supported by the New Energy and Industrial Technology Development Organization (NEDO) of Japan. The present work was in part financed by The Center for Surface Reactivity under the Danish Research Councils. Center for Atomic-Scale Materials Physics is sponsored by the Danish National Research Foundation.

References

[1] J.H. Sinfelt, *Bimetallic Catalysts: Discoveries, Concepts, and Applications* (Wiley, New York, 1983).

[2] V. Ponec, Adv. Catal. 32 (1983) 149.

[3] G.A. Somorjai, *Surface Chemistry and Catalysis* (Wiley, New York, 1994).

[4] N.T. Andersen, F. Topsøe, I. Alstrup and J.R. Rostrup-Nielsen, J. Catal. 104 (1987) 454.

[5] A.M. Schoeb, T.J. Raeker, L. Yang, T.S. King and A.E. DePristo, Surf. Sci. 278 (1992) L125.

[6] Y.L. Lam, J. Chiado and M. Boudart, Nouv. J. Chim. 1 (1977) 461.

[7] J.A. Rodriguez and D.W. Goodman, Science 257 (1992) 897.

[8] L. Pleth Nielsen, F. Besenbacher, I. Stensgaard, E. Lægsgaard, C. Engdahl, P. Stoltze, K.W. Jacobsen and J.K. Nørskov, Phys. Rev. Lett. 71 (1993) 754.

[9] F.R. de Boer, R. Boom, W.C.M. Mattens, A.R Miedema and A.K. Niessen, *Cohesion in Metals* (North-Holland, Amsterdam, 1988).

[10] T.P. Beebe Jr., D.W. Goodman, B.D. Kay and J.T. Yates, J. Chem. Phys. 87 (1987) 2305.

[11] A. Luntz and J. Harris, Surf. Sci. 258 (1991) 397.

[12] M.B. Lee, Q.Y. Yang and S.T. Ceyer, J. Chem. Phys. 87 (1987) 2724.

[13] P.M. Holmblad, J. Wambach and I. Chorkendorff, J. Chem. Phys. 102 (1995) 8255.

[14] H. Burghgraef, A.P.J. Jansen and R.A. van Santen, J. Chem. Phys. 101 (1994) 11012;
R.A. van Santen and M. Neurock, Concepts in theoretical heterogeneous catalytic reactivity, Catal. Rev., in press.

[15] H. Yang and J.L. Whitten, J. Chem. Phys. 96 (1992) 5529.

[16] O. Swang, J.K. Faegri, O. Gropen, U. Wahlgren and P.E.M. Siegbahn, Chem. Phys. 156 (1991) 379.

[17] P. Kratze, B. Hammer and J.K. Nørskov, J. Chem. Phys. (1996), submitted.

[18] M.C. Payne, M.P. Teter, D.C. Allan, T.A. Arias and J.D. Joannopoulos, Rev. Mod. Phys. 64 (1992) 1045.

[19] J.P. Perdew, J.A. Chevary, S.H. Vosko, K.A. Jackson, M.R. Pederson, D.J. Singh and C. Fiolhais, Phys. Rev. B 46 (1992) 6671.

[20] P.M. Holmblad, J. Hvolbæk Larsen and I. Chorkendorff, J. Chem. Phys. (1996), in press.

[21] J.R. Rostrup-Nielsen, J. Catal. 85 (1984) 31.

[22] I. Alstrup and M.T. Tavares, J. Catal. 139 (1993) 513.